JOURNAL OF MATERIALS SCIENCE 28 (1993) 5901–5908

Superplastic behaviour of fine-grained white cast irons

LI HONG, C. F. BURDETT
Department of Metallurgy and Engineering Materials, University of Strathclyde, Glasgow G1 1XN, UK

WANG YOUMING
Department of Metal Forming, University of Science and Technology Beijing, Beijing 100083, People's Republic of China

Superplastic behaviour of three hypo-eutectic white cast irons with different carbon contents was investigated at elevated temperatures. Hot and warm working, and rapid solidification technology (RST) were used to refine the coarse cementite structure. The resulting microstructure consisted of a mixture of small carbides and fine ferrite grains. Hot and warm working was found to be a successful method to refine the structure of white cast irons having a carbon content of less than 2.6%. Rapid solidification technology was the most promising process to refine high carbon (> 3.0%) cast irons. The refined white cast irons exhibited low flow stress and high strain-rate sensitivity in both tensile and compression in the temperature range 650–770 °C. Tensile elongation to failure of 300% was found for 3.0% C RST iron, 220%, 150% and 80% for 2.2%, 2.6% and 3.0% C hot and warm rolled cast irons, respectively.

1. Introduction

Superplasticity is the ability of metals and alloys to undergo extremely large elongations to failure. The large elongation, and the low flow stresses associated with this phenomenon, are being exploited to form complex shapes with significant savings in weight and cost [1].

There are two main types of superplastic behaviour, micrograin or microstructural superplasticity and transformation or internal stress superplasticity. The structural prerequisites for superplasticity are reasonably well understood. The principal microstructural feature required is a very fine grain size (< 10 μm). This requirement often necessitates the presence of a uniformly distributed, fine second phase to prevent grain growth at superplastic forming temperatures [2].

Several methods have been developed for the attainment of fine-grain superplastic structure, which include severe cold working followed by recrystallization, hot and warm working of cast billets, rapid solidification through powder metallurgy, thermal cycling through solid phase transformations, etc. [3, 4].

Superplasticity in metallic materials has been reviewed extensively, and many investigations have been carried out on the superplastic properties of aluminium-, titanium-, nickel-, and iron-based alloys [4]. However, only limited work has been published which considers the superplastic behaviour of white cast iron [5–8].

White cast irons are normally regarded as very brittle materials at all temperatures, owing to the presence of a large volume fraction of carbides which are distributed in a rather massive form within a ferrite matrix. Recent research has shown that white cast irons can exhibit superplasticity at elevated temperatures if the massive cementite can be effectively refined [9–13].

The purpose of this investigation is to obtain fine superplastic structures in white cast irons of three different compositions through (a) hot and warm working, and (b) powder metallurgy, using powder produced by rapid solidification technology (RST), and to evaluate their superplastic behaviour at elevated temperatures.

2. Experimental procedure

Three different compositions of white cast iron ingots were chosen in this study. The compositions are shown in Table I. To avoid graphitization, high manganese (1.5%) and chromium (1.5%) levels were selected and the silicon content was kept to a minimum.

The cast irons which were to be processed by hot working were air-melted at 1500 °C in a high-frequency induction furnace and poured into a 60 mm × 60 mm × 45 mm sand mould. The as-cast ingots were heated to 1100 °C for 3 h, and then forged to oblong blocks of approximately 22 mm in height, followed by air cooling. The forged pieces were further treated in the following two-stage process. First the

0022–2461

TABLE I Chemical composition (wt%) of white cast irons

	C	Cr	Mn	V	Si	S	P	Fe
1	2.20	1.50	1.51	0.12	0.40	< 0.005	< 0.005	Bal.
2	2.61	1.51	1.48	0.20	0.43	< 0.005	< 0.005	Bal.
3	3.00	1.53	1.33	0.06	0.42	< 0.005	< 0.005	Bal.

blocks were heated to 1100 °C and then continuously rolled with about 1.5–2 mm reduction per pass in a two-high 190 mm mill until the temperature reached approximately 700 °C. Nine passes were achieved. The second step of the process consisted of isothermally rolling the partially worked slabs at 700 °C. Rolling was carried out using a reduction of 0.5–1 mm per pass until a final thickness of about 1.5 mm was reached.

White cast iron powders having similar composition to white cast iron ingot 3 (3.0% C) was produced by nitrogen gas atomization. The RST powders were sieved to remove powder particles greater than 147 μm. The average powder particle size was approximately 70 μm, and the structure consisted of retained austenite and ledeburite which, upon annealing at 700 °C, developed a very fine microstructure of ferrite and cementite (1–2 μm).

Hot isostatic pressing was used to obtain fully dense compacts. The powders were placed in an evacuated cylindrical steel can (diameter 50 mm and height 90 mm) and warm isostatically pressed at a pressure of 150 MPa for 4 h at 720 °C. The compacts were then hot forged at 800 °C to produce 50% reduction followed by isothermal rolling at 720 °C to produce a strip of thickness 1.5 mm.

Tensile specimens, which have a rectangular cross-section (5.0 mm × 1.5 mm) with a gauge length of 15 mm, were spark machined from the isothermally rolled strips. Cylindrical shaped compression test samples (10 mm diameter and 15 mm height), were also spark machined from the as-cast ingots, forged blocks and powder compacts.

Superplastic tensile and compression tests were conducted in the temperature range 650–770 °C using an Instron machine at constant crosshead speed. Strain-rate change tests were carried out to determine the strain-rate sensitivity parameter as well as the strain–stress relationship.

Microstructural observation of specimens was conducted using Newphot-21 and Nikon optical micro-

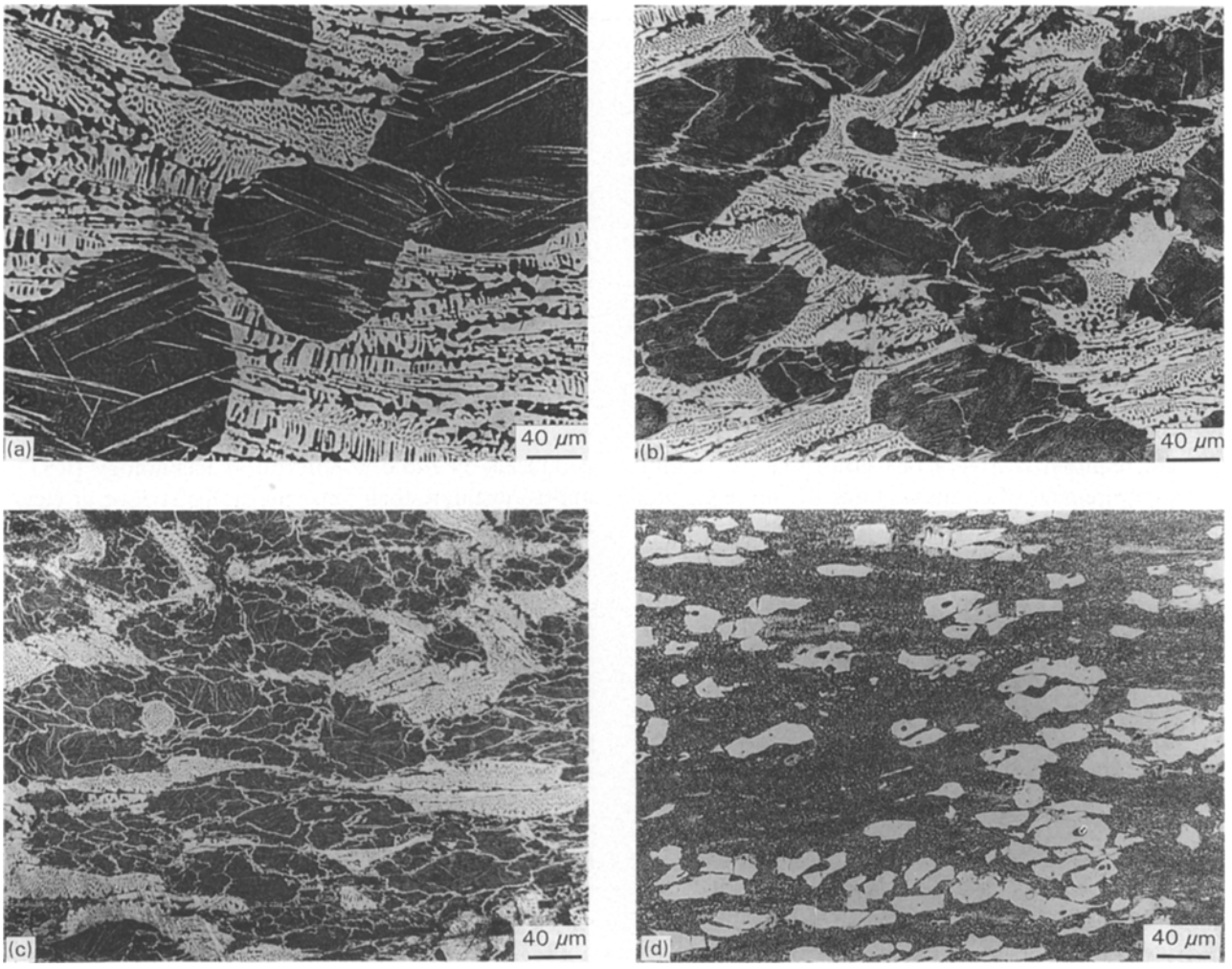

Figure 1 Optical micrographs of 3.0% C white cast iron for four different conditions: (a) as-cast; (b) hot forged; (c) hot rolled, and (d) warm rolled.

scopes and Jeol 350X and Philips 500 SEM microscopes. Transmission electron microscopy was used to compare the structures in the deformed region and the grip region of tensile samples.

3. Results

The results showed that white cast iron ingots containing between 2.2% and 3.0% C may undergo considerable hot deformation, and the resultant microstructure of the irons is determined by the thermomechanical process. Fig. 1 shows optical structures of 3.0% C white cast iron after four different processing conditions, i.e. as-cast, hot forged, hot rolled and isothermally warm rolled. The as-cast microstructure of hypoeutectic white iron consists of primary austenite dendrites which transformed to pearlite during cooling, with interdendritic areas of transformed ledeburite, which is the eutectic structure of cementite and pearlite (Fig. 1a). During the hot forging and hot rolling procedure the coarse cementite is refined (Fig. 1b, c). With increasing reduction and, more particularly, during the isothermal rolling process, the massive cementite is further refined, but there are still some carbide particles with a size greater than 10 μm (Fig. 1d).

Scanning electron micrographs of 3.0% C RST white cast iron are shown in Fig. 2. The as-received powders have a typical dendritic structure (Fig. 2a). X-ray diffraction measurement shows that retained austenite in the form of dendrites is the main microstructural constituent and the interdendritic phase is ultrafinely dispersed carbide. During the hot isostatic pressing process at 720 °C, the metastable retained austenite within the powder quickly transforms to stable ferrite and carbide, so that the structure of compacts consists of areas of ferrite of grain size 1–2 μm together with a fine carbide (0.1–2 μm) (Fig. 2b).

Tensile stress–strain curves are presented in Fig. 3 for both hot and warm rolled cast irons and rapidly solidified cast iron tested at 700 °C at an initial strain

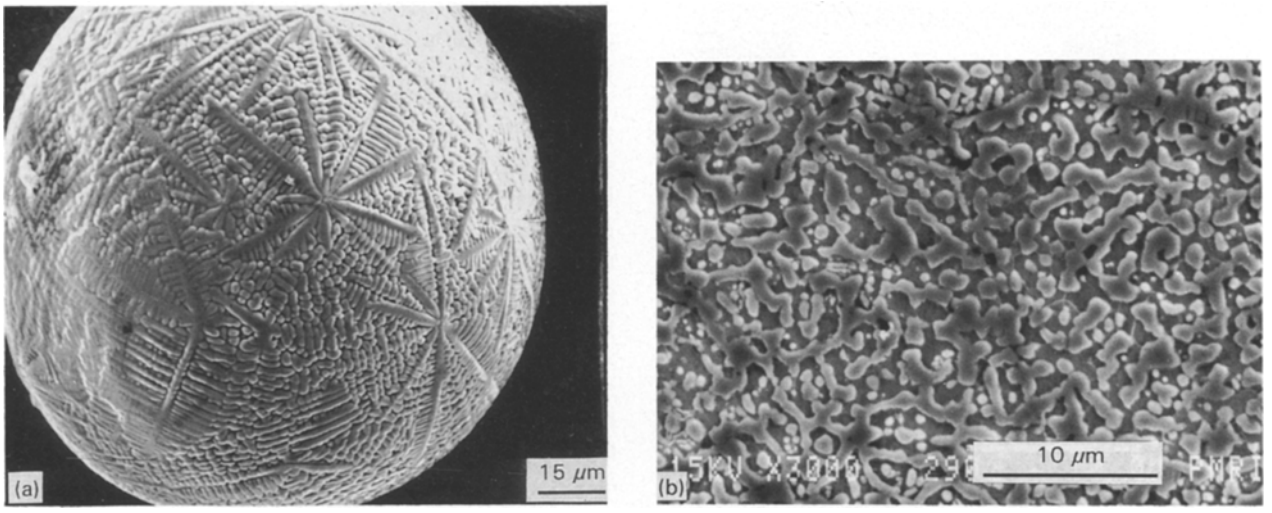

Figure 2 Scanning electron micrographs of RST–3.0% C white cast iron: (a) morphology of powder; (b) powder compact hot pressed at 720 °C.

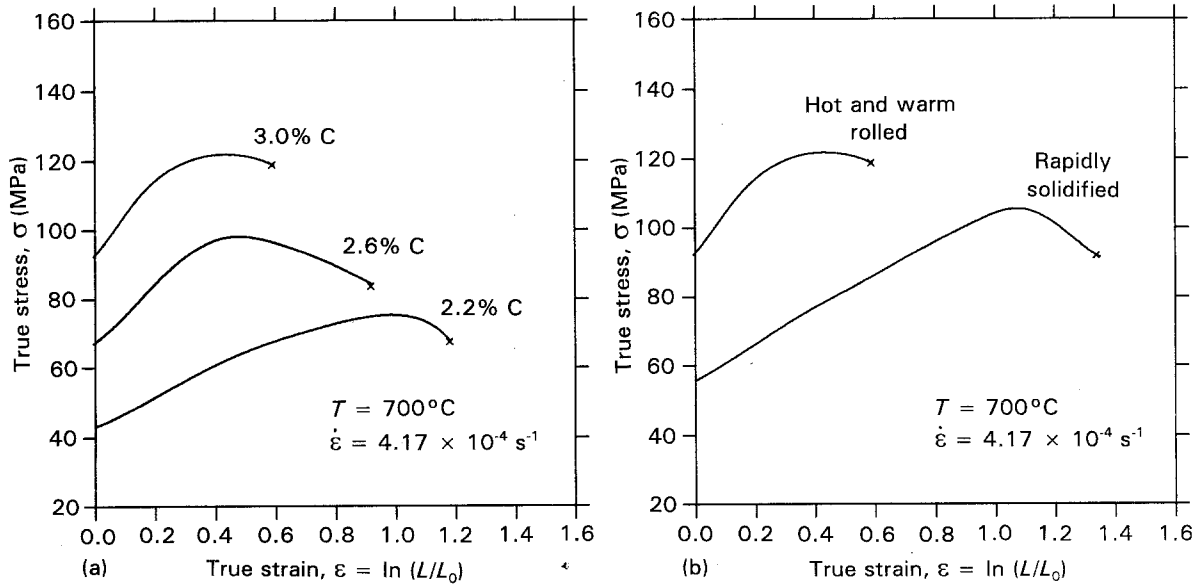

Figure 3 Stress versus strain in tensile tests: (a) hot and warm rolled samples; (b) RST processed sample.

rate of $4.17 \times 10^{-4}\,s^{-1}$. It is readily seen in Fig. 3a that the value of elongation to failure and the flow stress for hot and warm rolled samples increases with decreasing carbon content in cast iron. Elongations to failure of 220%, 150% and 80% were found for the 2.2%, 2.6% and 3.0% C specimens, respectively (Fig. 4a). However, under the same testing condition, the 3.0% C RST sample had an elongation of 300% (Fig. 4b). There is a dramatic decrease in flow stress compared with the hot and warm rolled sample (Fig. 3b).

True stress–true strain curves in compression at 700 °C for the 3.0% C white cast iron processed by as-cast, hot forged and rapidly solidified methods are given in Fig. 5. All tests were performed at an initial

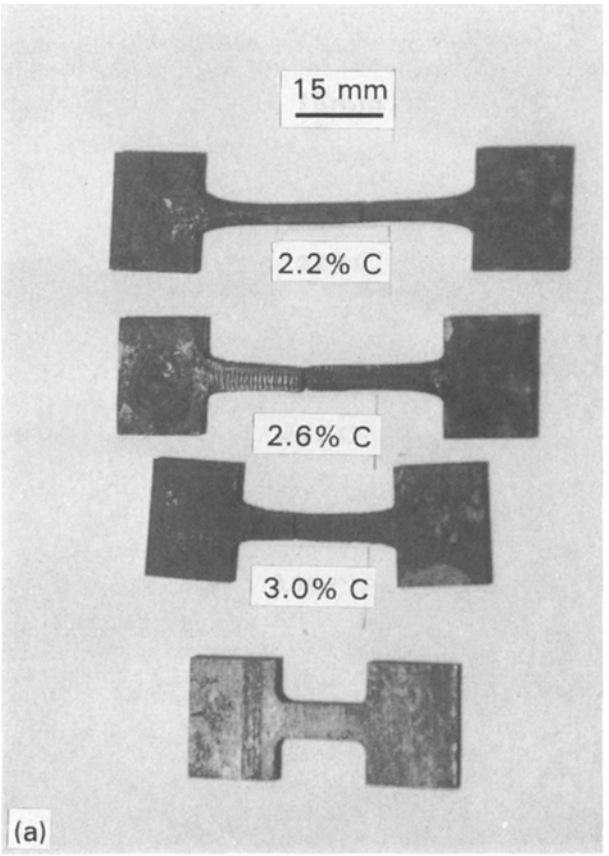

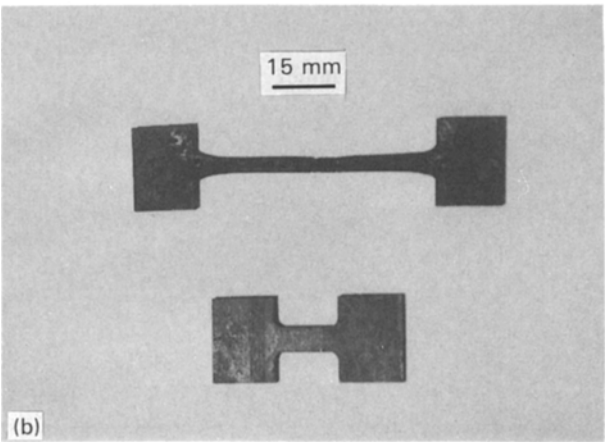

Figure 4 Photograph of a tensile sample tested at 700 °C and initial strain rate of $4.17 \times 10^{-4}\,s^{-1}$: (a) hot and warm rolled samples; (b) RST processed sample.

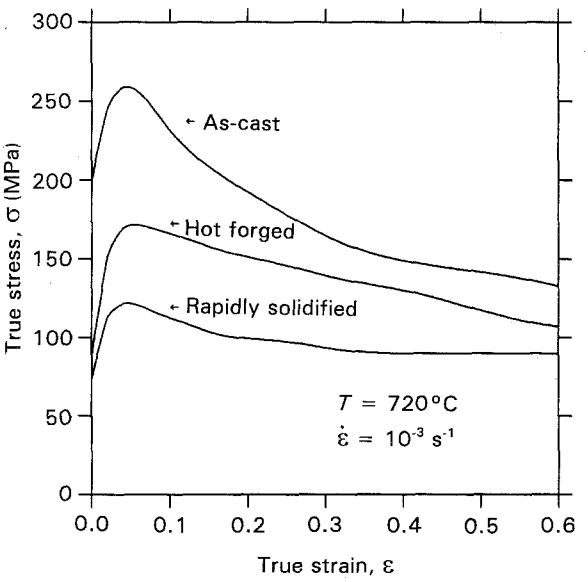

Figure 5 Stress versus strain for 3.0% C white cast iron samples in a compression test.

strain rate of $1.0 \times 10^{-3}\,s^{-1}$. The flow stress is seen to decrease in the following order of processing histories: as-cast, hot forged, and RST compacted powder, i.e. the finer the cementite, the lower is the flow stress.

A typical practice of determining the flow stress–strain rate relation from a single test is to perform strain-rate change tests. In this study, samples were first predeformed at a given strain rate to a true strain of 0.2–0.3 before strain-rate changes, which can minimize the effect of grain growth on stress versus strain rate. A set of strain-rate change tests in tension was performed on the three hot and warm rolled samples and RST–3.0% C samples in the temperature range 650–750 °C. The results are shown in Fig. 6 in the form of a double logarithmic plot of true stress as a function of true strain rate. The strain-rate sensitivity, m, is calculated using the equation

$$m = \log(\sigma_1/\sigma_2)/\log(\dot{\varepsilon}_1/\dot{\varepsilon}_2) \quad (1)$$

Stress versus strain rate for RST 3.0% cast iron tested at three different temperatures is plotted in Fig. 6a. The highest strain-rate sensitivity exponent, $m = 0.5$, was calculated for this material at 700 °C in the low stress and low strain-rate region (Region II). At high stress and high strain rate (Region III), m lies between 0.1 and 0.2. It is noted that material containing γ + cementite (750 °C) is a little stronger than material containing α + cementite (700 °C) at low strain rates, while at high strain rates the opposite is found.

The results of three hot and warm rolled cast irons tested at 700 °C are given in Fig. 6b. The value of m decreases with increasing carbon content. At a particular strain rate, its flow stress increases with increasing carbon content. The difference between cast iron produced by hot-warm rolling to that produced by RST method for 3.0% C white cast iron tested at 700 °C is shown in Fig. 6c. There is a higher m value in the RST sample than in the hot-warm rolling one in all the testing regions.

Strain-rate change tests were also carried out in compression for RST 3.0% cast iron at three different

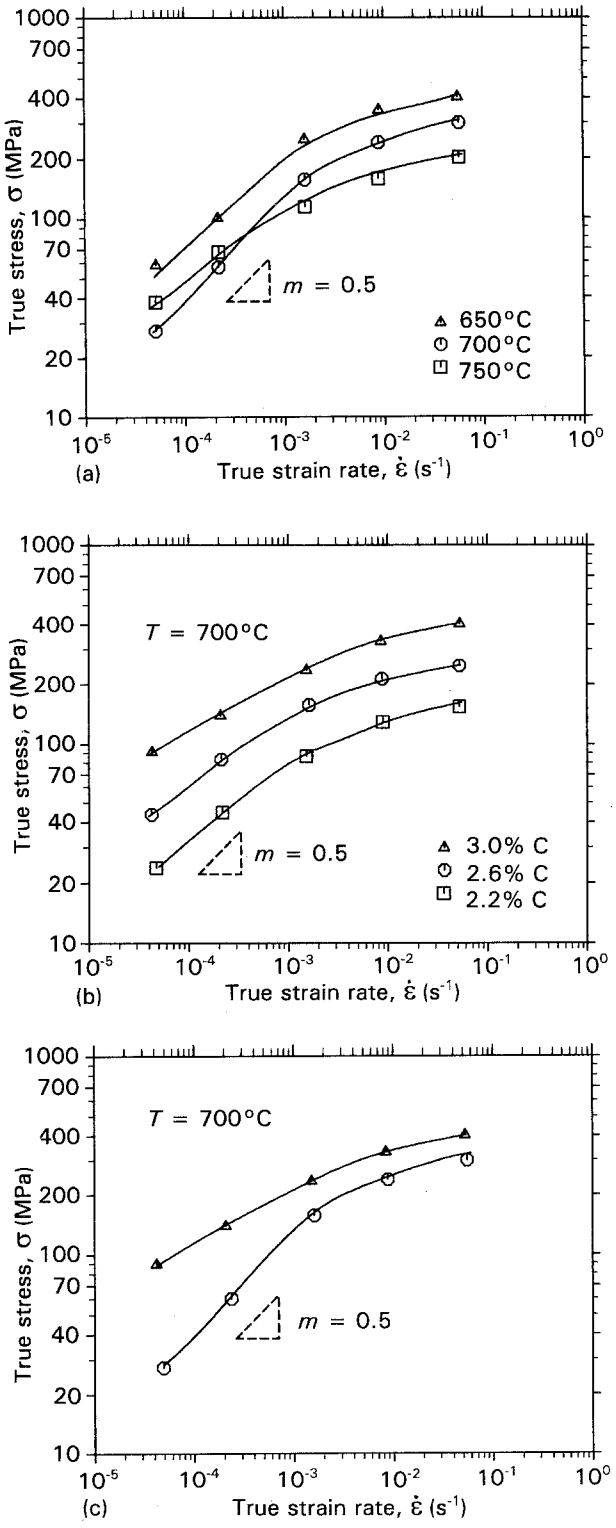

Figure 6 Stress versus strain rate obtained from strain-rate change in a tensile test: (a) RST samples; (b) hot and warm rolled samples; (c) 3.0% C cast iron samples. (a) (△) 650 °C, (○) 700 °C, (□) 750 °C. (b) (△) 3.0% C, (○) 2.6% C, (□) 2.2% C. (c) (△) hot and warm rolled, (○) rapidly solidified.

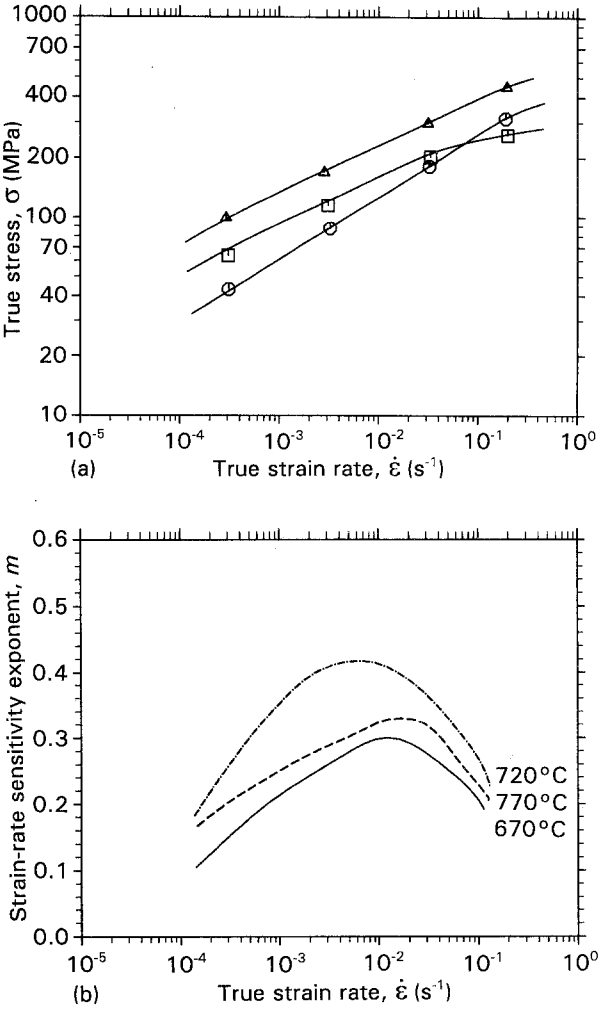

Figure 7 Strain-rate change test results for 3.0% C RST samples in compression: (a) stress versus strain rate; (b) m versus strain rate. (a) (△) 670 °C, (○) 720 °C, (□) 770 °C.

temperatures. The results are shown in Fig. 7a and b in the form of true stress and strain-rate sensitivity, m, versus true strain rate, respectively. At 720 °C a maximum m value of 0.42 was obtained at strain rate of $2.0 \times 10^{-2}\,s^{-1}$ which is close to the commercial forming rate. This ultrafine-grained cast iron exhibits a low flow stress over a wide range of strain rates (Fig. 7a). The results supply a set of useful data for the near net shape forming of fine grain white cast irons.

4. Discussion

Microstructural analysis indicated that hot and warm working is a successful way to refine the coarse eutectic carbide in white cast iron. Through hot and warm rolling the final structure of white cast iron consists of small refined cementite particles distributed in a matrix of ferrite (Fig. 8). However, it is also noted that this thermal mechanical processing does not result in a uniformly fine distribution of carbides for high carbon content white cast iron, especially for 3.0% C cast iron. This is because higher carbon cast iron has a larger fraction of coarse eutectic carbide which is not readily refined by hot and warm working. Thus, the resultant microstructure is a mixture of fine carbides and ferrite grains with some large (> 10 μm) eutectic carbides (Fig. 8c).

The influence of carbon content on the flow stress and strain-rate sensitivity for hot and warm working cast irons (Fig. 3a) can be attributed to two factors. One is the pre-eutectic cementite particle size. As mentioned above, the thermomechanical processing does not result in a uniformly fine distribution of cementite in white cast irons. The higher the carbon content, the larger the eutectic carbide particle. These large cementite particles usually lead to cavitation at the interface and limit superplastic flow. The second factor is the difference in cementite fraction. It is well

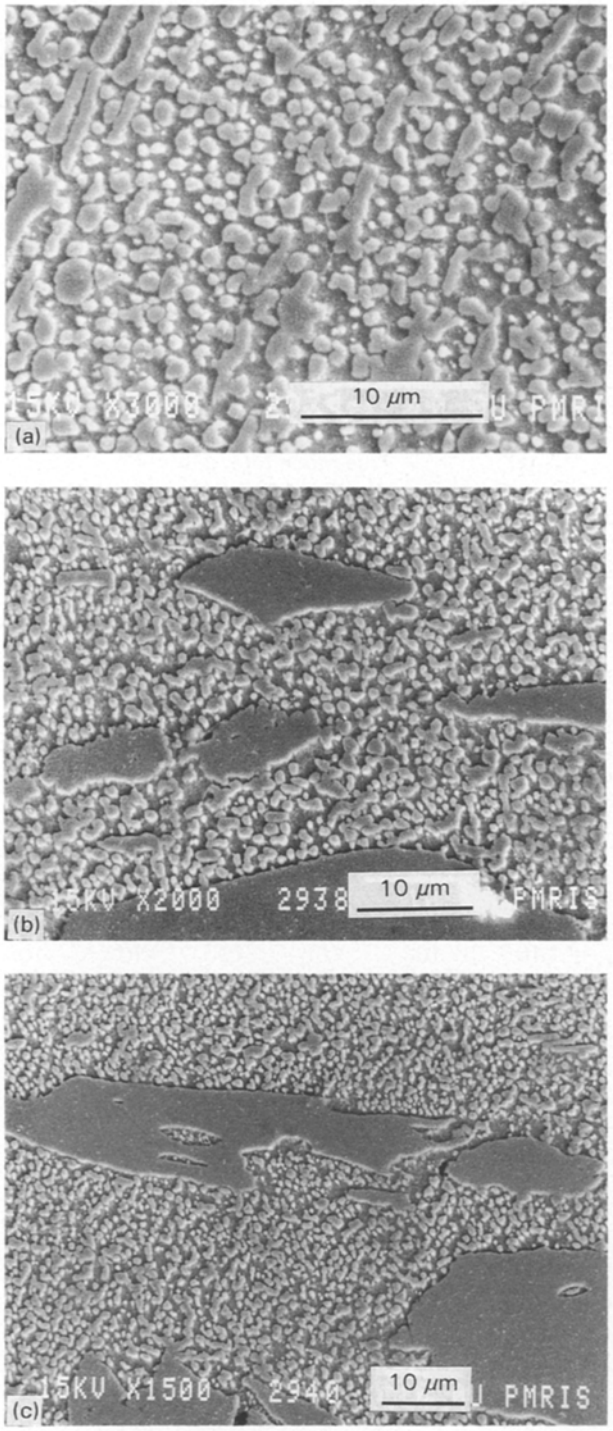

Figure 8 SEM microstructure of hot and warm rolled white cast irons: (a) 2.2% C; (b) 2.6% C; (c) 3.0% C.

known that cementite phase is stronger than ferrite phase at the same temperature. Thus the 3.0% C cast iron having a larger carbide particle size and more cementite fraction when compared to the 2.2% and 2.6% C cast irons, showed a higher strength and a lower tensile ductility and strain-rate sensitivity.

RST is proved to be the most promising method to refine high carbon content white cast irons because this powder metallurgy approach produces ultrafine-grained superplastic structure. There are no large eutectic carbides existing in 3.0% C RST cast iron (Fig. 2b) and this material showed very impressive elongation to failure of 300% and low flow stress at elevated temperatures.

All of the stress–strain curves shown in Figs 3 and 5 exhibit considerable strain hardening. This is believed to be due principally to grain growth occurring during superplastic flow. As is well documented in the literature [7], superplastic materials show a strong dependence of flow stress on grain size. Investigations using TEM on tensile deformed samples show that some ferrite grain growth occurred during superplastic flow. Fig. 9 shows TEM microstructures of the deformed region and the grip region (no strain) for RST–3.0% C sample after tensile elongation of 100% with an initial strain rate of $4.17 \times 10^{-4} s^{-1}$ at 700 °C. Ferrite grain growth in the deformed region (Fig. 9a) is obviously observed compared with that in the grip region (Fig. 9b).

Analysis of the superplastic fracture surfaces using optical and SEM shows that the mode of deformation near fracture was quite different for hot-warm rolled and RST processed samples. Fig. 10 illustrates this difference for two 3.0% C materials after testing at 700 °C. The hot-warm rolled material shows extensive cavitation at or near the large eutectic carbides (Fig. 10a, b). The RST material, on the other hand, shows virtually no cavitation (Fig. 10c, d). These results confirm the importance of a fine microstructure in the high-temperature ductility and fracture of materials at intermediate temperatures.

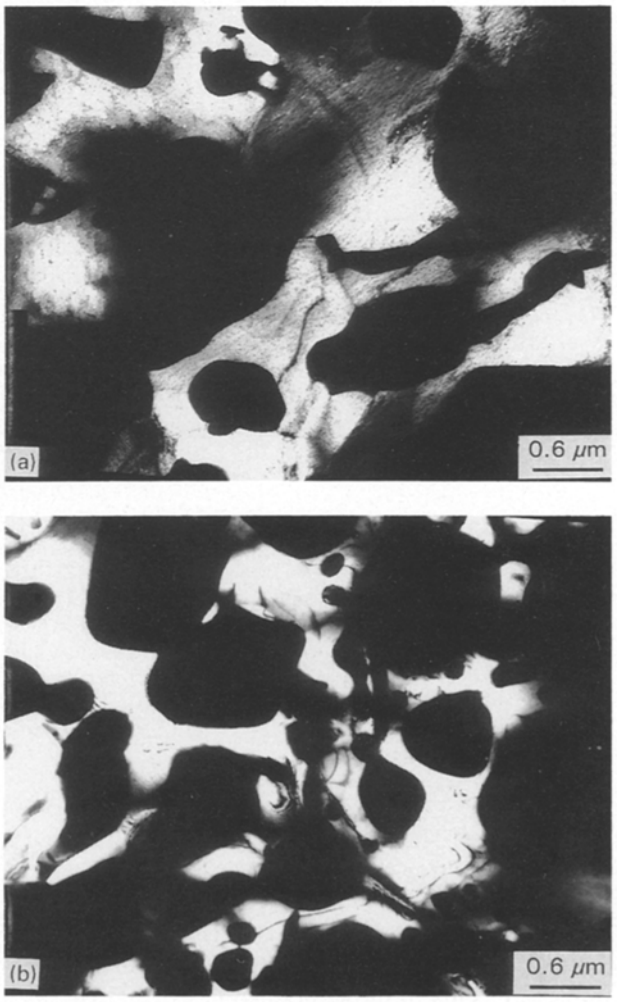

Figure 9 TEM microstructure for 3.0% C RST tensile samples deformed at 700 °C and $\dot{\varepsilon} = 4.17 \times 10^{-4} s^{-1}$: (a) deformed region (100% elongation); (b) grip region.

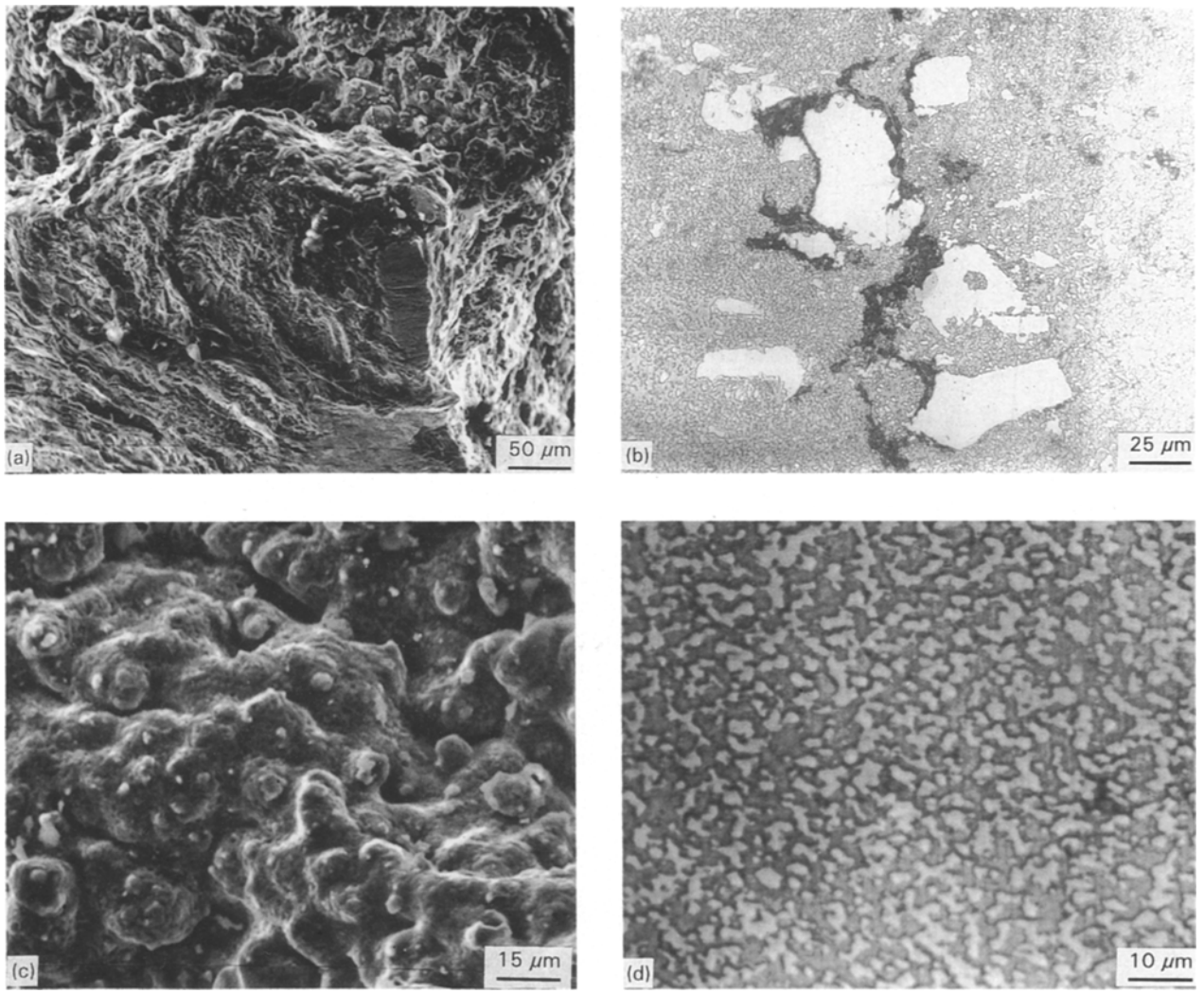

Figure 10 Fracture surface of 3.0% C tensile samples deformed at 700 °C and $\dot{\varepsilon} = 4.17 \times 10^{-4}\,s^{-1}$: (a) hot and warm rolled sample (SEM); (b) hot and warm rolled sample (LM); (c) RST sample (SEM); (d) RST sample (LM).

All of the stress–strain rate curves exhibited a sigmoidal shape typical of most superplastic materials using the normal nomenclature. At low strain rates (Region II), the strain-rate sensitivity exponents, m, were approximately 0.5 (i.e. $n = 2$). In this region, grain-boundary sliding is believed to be the rate-controlling process in plastic flow. At high strain rates (Region III), the strain-rate sensitivity exponents, m, were low and approached values in order of 1/6 to 1/8 (i.e. $n = 6$–8). In this region deformation by slip processes involving dislocation climb is believed to be the rate-determining step for plastic flow.

The above results suggest that the creep-rate of white cast irons can be correlated by means of two additive contributions to plastic flow, namely

$$\dot{\varepsilon} = \dot{\varepsilon}_{spf} + \dot{\varepsilon}_{sc} \quad (2)$$

where $\dot{\varepsilon}_{spf}$ is the creep rate associated with superplastic flow and $\dot{\varepsilon}_{sc}$ is the creep rate associated with slip creep. Specific expressions have been developed to describe these relations. The superplastic flow rate of fine grain sized materials, when grain-boundary diffusion is rate controlling [3, 14], is given by

$$\dot{\varepsilon}_{spf} = A\frac{\boldsymbol{b}D_{gb}}{d^3}\left(\frac{\sigma}{E}\right)^2 \quad (3)$$

where $A = 10^8$, d is the grain size, $\boldsymbol{b}$ is Burgers vector, D_{gb} is the grain-boundary diffusion coefficient in the matrix phase of the superplastic materials, σ is the creep stress, and E is the unrelaxed dynamic Young's modulus. The creep rate in the slip creep range, where lattice diffusion is rate controlling, is given by [15]

$$\dot{\varepsilon}_{sc} = A'\left(\frac{\lambda}{\boldsymbol{b}}\right)^3\frac{D_L}{\boldsymbol{b}^2}\left(\frac{\sigma}{E}\right)^8 \quad (4)$$

where $A' = 10^9$ for high stacking fault energy materials, λ is the subgrain size or barrier spacing (in the case of the white cast irons the grain size or the interparticle spacing whichever is the finest), and D_L is the lattice self-diffusion coefficient.

The stress exponent, n, and the activation energy, Q, for creep can be calculated from the equation

$$\dot{\varepsilon} = K\exp(-Q/RT)\sigma^n \quad (5)$$

where K is a materials constant, R is the gas constant, and T is the temperature. From this equation, n can be obtained by determining the slope of log $\dot{\varepsilon}$ versus log σ, and the activation energy can be calculated from

$$Q_{|\sigma = \text{constant}|} = -R\frac{d\ln\dot{\varepsilon}}{d(1/T)} \quad (6)$$

Using the strain rate and stress data in Fig. 6a and Equation 6, the strain rate, $\dot{\varepsilon}$, as a function of reciprocal temperature, $1/T$, is given in Fig. 11. The slope of the curves is used to determine the activation energy, Q, for superplastic deformation. As can be seen, at constant stresses of 70 and 90 MPa the activation energies for plastic flow in the superplastic region (Region II) are about 164 and 179 kJ mol^{-1}, respectively. These values are nearly identical to the grain-boundary self-diffusion activation energy in alpha iron, 170 kJ mol^{-1}. At constant stresses of 230 and 250 MPa the activation energies for plastic flow in the slip creep region (Region III) are approximately 263 and 274 kJ mol^{-1}, respectively, which are close to the observed activation energy for lattice self diffusion of iron (252 kJ mol^{-1}).

The strength difference in tension of the 3.0% C RST cast iron above A_1 (750 °C) and below the A_1 (700 °C) is readily seen in Fig. 6a. At low strain rates, the austenite phase material (750 °C) is slightly stronger than the ferrite phase material (700 °C) in the superplastic region; this can be attributed to a grain-size difference, because grain growth is likely to be enhanced in the austenite region as there is less cementite present than in the ferrite region. At high strain rates in the slip creep region, the ferrite phase material is stronger than the austenite material. Several factors can contribute to the latter observation. First, the barrier spacing (i.e. the interparticle spacing and the grain size) in the ferrite range is probably smaller than in the austenite; if Equation 4 is used to predict the difference in barrier spacing from the difference in strength, about a factor of two is calculated. This is the most likely factor influencing the difference in strength at high strain rates. A second factor is that the solid-solution hardening (e.g. atom size differences) contribution of manganese and other elements may be more effective in the ferrite than in the austenite phase. A third factor is the possible contribution of the hardness of cementite to the strength of the iron–cementite composite in the 3.0% C RST cast iron samples. That is, it is known that the hardness of cementite is an order of magnitude higher than the hardness of alpha iron at 700 °C but is only a factor of two harder than gamma iron when the hardness data are extrapolated to 750 °C. The strength difference in compression of this material (Fig. 7a) above and below A_1 is also probably caused by the above-mentioned factors.

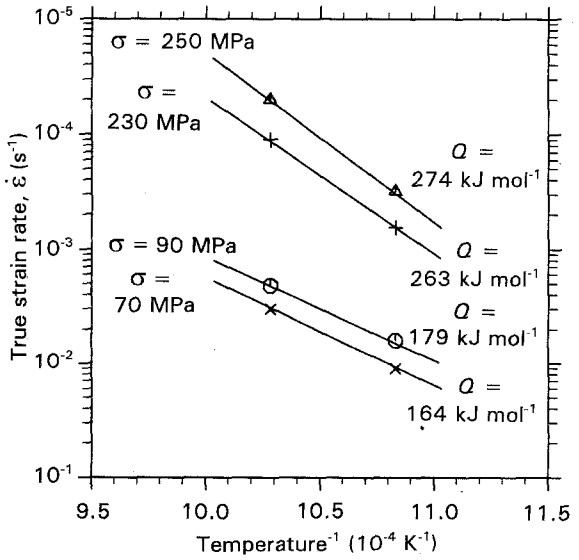

Figure 11 Strain rate, $\dot{\varepsilon}$, as function of reciprocal temperature, $1/T$; the slope of the curves is used in determination of activation energy for superplastic deformation.

5. Conclusion

The structure of white cast irons can be effectively refined through hot and warm working and rapid solidification technology. Hot and warm working is a successful method to refine the structure of white cast irons having a carbon content of less than 2.6%. Rapid solidification technology is the most promising way to refine high carbon (> 3.0%) cast irons.

The refined white cast irons exhibit good superplasticity in both tensile and compression in the temperature range 650–770 °C. Tensile elongation to failure of 300% was found for 3.0% C RST iron, 220%, 150% and 80% for 2.2%, 2.6% and 3.0% C hot and warm rolled cast irons, respectively.

At low flow stresses, the RST–3.0% C white cast irons show a high strain-rate sensitivity exponent $m = 0.42$–0.5 in both tensile and compression tests.

The optimum condition for superplastic deformation for this material is a temperature of 700–720 °C and a strain rate of 10^{-3}–$2.0 \times 10^{-2}\,s^{-1}$.

References

1. H. C. HEIKKENEN and T. R. MCNELLEY (eds), "Superplasticity in Aerospace" (The Metallurgical Society, Warrendale, PA, 1988).
2. N. E. PATON and C. H. HAMILTON (eds), "Superplastic forming of structural alloys" (TMS AIME, Warrendale, PA, 1982).
3. O. D. SHERBY and J. WADSWORTH, in "Deformation, processing and structure", edited by G. Kraus (ASM, Metals Park, OH, 1984) pp. 355–88.
4. J. PILLING and N. RIDLEY, "Superplasticity in Crystalline" (The Institute of Metals, London, 1989).
5. J. WADSWORTH and O. D. SHERBY, *Foundry MT* **106** (1978) 59.
6. J. WADSWORTH, L. E. EISELSTEIN and O. D. SHERBY, *Mater. Eng. Appl.* **1** (1979) 143.
7. O. A. RUANO, L. E. EISELSTEIN and O. D. SHERBY, *Metall. Trans.* **13A** (1982) 1785.
8. G. FROMMEYER, in "7th International Conference on the Strength of Metals and Alloys" (ICSMA7), Montreal, Canada, 12–16 August, 1985, Vol. 2, edited by H. J. McQueen, J. P. Bailon, J. I. Dickson, J. J. Jonas and M. G. Akben (Pergamon, 1985) pp. 877–84.
9. D. BURCHARD, K. U. KAINER and B. L. MORDLIKE, *ibid.*, Vol. 2, pp. 1645–50.
10. LI HONG, WANG YOUMING and C. B. BURDETT, *Mater. Sci. Technol.* **7** (1991) 660.
11. WANG YOUMING and LI HONG, *Iron Steel (China)* **23** (1988) 31.
12. H. J. SPEIS and G. FROMMEYER, *Mater. Sci. Technol.* **7** (1991) 718.
13. WANG YOUMING and LI HONG, *J. Beijing Univ. Iron Steel Technol.* **10** (1988) 330.
14. B. WALSER and O. D. SHERBY, *Met. Trans.* **10A** (1979) 1461.
15. O. D. SHERBY, R. H. KLUNDT and A. K. MILLER, *ibid.* **8A** (1977), 843.

Received 16 February
and accepted 16 April 1993